Fourier Methods in CT: projection and reconstruction algorithms

Silvia De Francesco and Augusto Silva
IEETA/DET Universidade de Aveiro, Campus Universitario, 3810 Aveiro, Portugal
silvia@ieeta.pt, asilva@ieeta.pt

Abstract **– Related to the demand for 3D reconstruction, the interest for Fourier reconstruction methods has been growing due to their reduced computational complexity.**
In this paper we are going to review the application of Fourier theory to the field of tomography, both for projection and reconstruction. Some Fourier reconstruction methods are described including NUFFT based methods both for parallel and for divergent projections.

Resumo **– Recentemente, devido à crescente exigência de reconstrução em 3D, o interesse para os métodos de reconstrução baseados na teoria de Fourier tem aumentado dada a reduzida complexidade computacional. Neste artigo revê-se a aplicação da teoria de Fourier à tomografia, tanto em reconstrução como em projecção. São descritos e comparados alguns métodos de Fourier entre os quais métodos baseados em NUFFT para projecções paralelas e divergentes.**

Keywords **– Computed tomography, tomographic reconstruction algorithms, direct Fourier methods, sinogram, rebinning, NUFFT.**

Palavras chave **– Tomografia computorizada, algoritmos de reconstrução tomográfica, métodos directos de Fourier, sinograma, "rebinning", NUFFT.**

I. Introduction

Tomographic projection and reconstruction processes are based on a common framework in which Fourier theory, with the well known Fourier Slice Theorem (which states the relation between the Fourier transform of parallel projections and the 2D Fourier transform of the object cross section), plays a central role. Moreover, a special class of reconstruction methods, known as Direct Fourier (or Fourier-based) methods, stems directly from this theory.

The first Fourier-based reconstruction method was described in 1956 by Bracewell. Since then, many Fourier-based methods have been developed, both for projection and reconstruction but their usage has been limited due to the advent of methods like FBP –Filtered Back-Projection– which, in spite of the higher computational complexity –$O(N^3)$ operations–, allows for the execution of reconstruction in pipe-line with the acquisition process and gives better quality results.

Nowadays, with the advent of technologies like spiral CT, the reconstruction process is performed a posteriori (after the acquisition process is completed) and the comparison between different reconstruction methods is based just on computational complexity and image quality.

With the use of FFT –Fast Fourier Transform– algorithm, Fourier-based reconstruction methods turned out to be the fastest now available –$O(N^2 \log N)$ operations–, being suitable for 3D reconstruction. The interest for these methods has been growing and Fourier-based reconstruction methods have been developed which are able to compete with FBP method in what concerns reconstructed image quality.

In the proposed paper we review the application of Fourier theory to the field of tomography, both for projection and reconstruction. We address the basics of direct Fourier methods as well as some specific implementations.

In section II the basics of tomography are briefly described, a complete and rigorous approach to this field can be found in [1], [2] and [3].

Section III deals with the standard direct Fourier method, which suffers from distortion, but can be improved by applying techniques like zero-padding, and with a NUFFT-based direct Fourier method.

Fourier methods are not directly suitable for divergent projections, this means that in order to be applied to the real data (which normally are taken with divergent geometry) a rebinning step has to be performed. This procedure, as well as a new NUFFT-based method applied to the divergent projections are described in section IV.

In section V, the Fourier based projection process is briefly described and, finally, in section VI a few results are shown, comparing the quality of the reconstructed images.

II. Basics of tomography

The distribution of a parameter on a transversal section of an object can be modeled as a 2D function f (object function) in the (x, y) plane of the section. In most of the applications (medical, for example), the function f is limited in space, which means that it vanishes outside a finite region of the plane.

The two parameters θ (slope of the line $+\frac{\pi}{2}$) and s (distance to the center of rotation) univocally specify the line with equation

$$x\cos\theta + y\sin\theta = s \tag{1}$$

in the (x, y) plane and the general formula for the line integral, known as the Radon transform of $f(x, y)$, is:

$$p(\theta, s) = \iint f(x, y)\delta(x\cos\theta + y\sin\theta - s)dxdy \tag{2}$$

A projection consists of a collection of integrated values of $f(x, y)$ taken along a set of straight lines in the plane and the projection data set is given by a number of projections taken with different orientations. Basically, two geometries have been defined for the sets of line integrals making a 2D projection: parallel and divergent (or fan-beam).

In parallel geometry (historically, the first to be used), a projection $p_\theta(s)$ consists of a collection of line integrals (2) taken along straight parallel lines in the plane, that means, a collection of $p(\theta, s)$ with constant θ (fig. 1) and $s \in \left[-\frac{S}{2}, \frac{S}{2}\right]$.

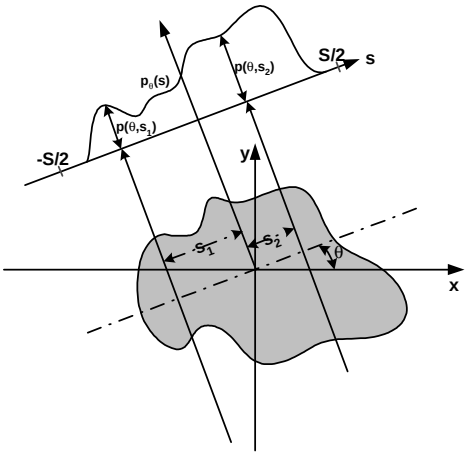

Figura 1 - An object $f(x, y)$ and its paralel projection $p_\theta(s)$.

In divergent geometry, to each angular position of the focus corresponds a fan of focus-detector lines (the detector being an array of detector elements). In this case, each line is defined by a pair of parameters (β, γ), where β is the slope of the central line of the beam $+\frac{\pi}{2}$ and γ is the angular offset of the line relative to the central one (fig. 2). Being Γ the fan-angle and r the focus-center of rotation distance, the equation of the line is

$$x\cos(\beta + \gamma) + y\sin(\beta + \gamma) = -r\sin\gamma \tag{3}$$

and each divergent projection is described by the formula:

$$\begin{aligned} p_\beta(\gamma) \quad = \quad & \iint f(x, y)\delta(x\cos(\beta + \gamma) + \\ & y\sin(\beta + \gamma) + r\sin\gamma)dxdy \end{aligned} \tag{4}$$

with constant β and $\gamma \in \left[-\frac{\Gamma}{2}, \frac{\Gamma}{2}\right]$.

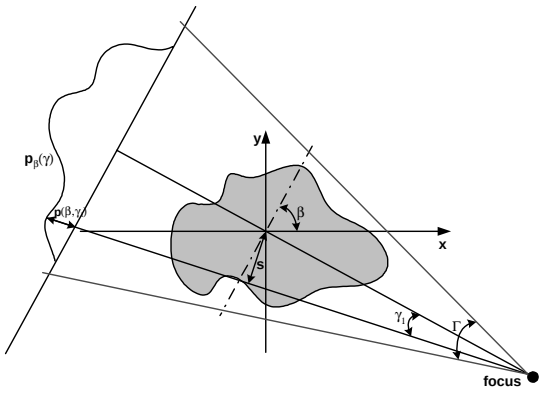

Figura 2 - An object $f(x, y)$ and its fan-beam projection $p_\beta(\gamma)$.

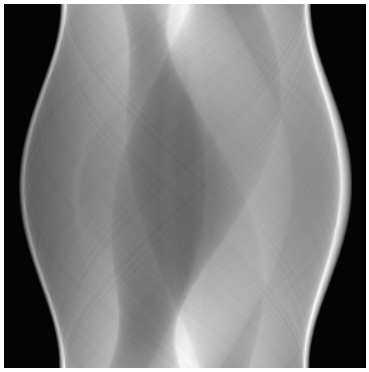

Figura 3 - Sinogram of Modified Shepp-Logan phantom: 256 projections over 180º, 255 rays.

In Radon space (θ, s), the space of $f(x, y)$ Radon transform, a projection data set for a given geometry corresponds to a set of samples taken over a specific sampling grid. A projection data set for parallel geometry, called sinogram, is a 2D matrix (fig. 3) where to each row corresponds a value for the parameter θ (a parallel projection), and to each column a value for the parameter s.

Similarly, a projection data set for a divergent geometry is a 2D matrix where to each row corresponds a value for the parameter β (a divergent projection) and to each column a value for the parameter γ.

A. Fourier Slice Theorem

The Fourier slice theorem (see [1] for details and demonstration) states that:

Theorem 1: The Fourier transform of a parallel projection of an object function $f(x, y)$ taken at angle θ gives a slice of the two dimensional transform of $f(x, y)$, $F(u, v)$, subtending an angle θ with the u axis.

In other words, the 1D Fourier transform $P_\theta(\sigma)$ of the parallel projection $p_\theta(s)$, gives the values of $F(u, v)$ along line BB in figure 4.

III. Fourier reconstruction methods for parallel projections

The Fourier slice theorem suggests a simple way to solve the reconstruction problem. Taking parallel pro-

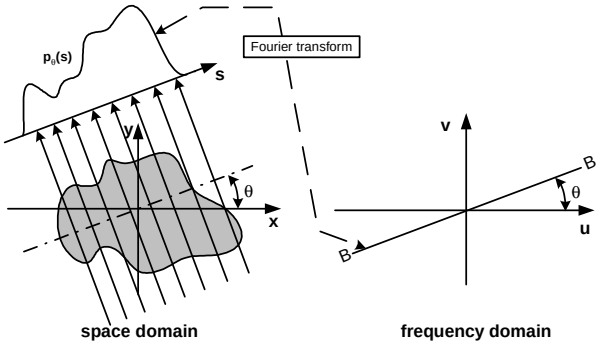

Figura 4 - Graphic visualization of Fourier slice theorem statement.

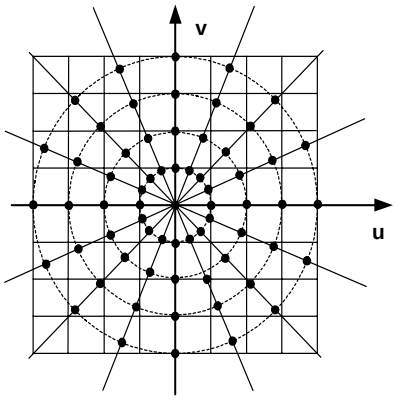

Figura 5 - Sample points on a conventional polar grid and cartesian grid.

jections of the object function f at angles θ_1,θ_2,...θ_n and Fourier transforming each of them, we obtain the 2D Fourier transform of the object function $F(u, v)$ on n radial lines. In ideal conditions (infinite number of projections and samples per projection) $F(u, v)$ would be known at all points in the frequency domain and the object function $f(x, y)$ could be recovered by 2D inverse Fourier transforming $F(u, v)$.

Fourier reconstruction methods (also known as direct Fourier or Fourier based methods) follow directly from this ideal procedure, adapted to the discrete case.

In practice, only a finite number of projections and samples per projection are taken and $F(u, v)$ is known just on a finite number of points along a finite number of radial lines (5-a) and, in order to obtain an approximation of $f(x, y)$ by 2D inverse Fourier transform of $F(u, v)$, we have to interpolate from the radial points to the points on a Cartesian grid. Basically, Fourier reconstruction methods are three steps methods:

- 1D discrete Fourier transform (through FFT algorithm) of the parallel projections taken at n angles θ_1,θ_2,...θ_n
- Polar to Cartesian grid interpolation
- 2D inverse Fourier transform (again, using FFT).

Unfortunately, the results of such a straight method suffer from artifacts due to interpolation in Fourier plane and to aliasing (since function $f(x, y)$ is not band limited). Various techniques have been proposed in order to improve the performance of this method giving rise to a class of methods known as Direct Fourier (DFM). Some methods are based on peculiar sampling schemes – polar interleaved grid [4], polar square grid [Pasciak] [5], linogram [6]–, while some others take advantage of recent developments in the calculation of FFT for Non Uniformly distributed samples (NUFFT) [7] [8]. Moreover, all of them apply classical signal processing techniques like zero-padding of the projections (which gives a denser set of samples in the Fourier domain) or gridding in Fourier space (which means to interpolate over a denser cartesian grid) in order to avoid aliasing.

While improving image quality, the former techniques deteriorate the computational performance of the algorithm. We've implemented and compared some of these methods in what concerns image quality, reconstruction time and performance in presence of noise.

A. Classical Direct Fourier Method

Comparing the polar and the Cartesian grids in figure 5, we see that, close to the origin (where most of the frequency information is concentrated), the polar samples are separated by a smaller angular distance compared to the radial distance meaning that interpolation error is bigger in the radial than in the angular direction. This fact has suggested that a higher order filter should be used in the radial direction. For instance, Low and Natterer [5] suggest to apply nearest neighbour interpolation in the angular direction and a modified sinc interpolation filter to the sample set with double density in the radial direction (obtained by zero-padding of the sinogram).

Our implementation follows the three basic steps of DFM, and takes advantage of the Matlab function *interp2* which performs two dimensional cubic interpolation in a very efficient way. Moreover, in order to avoid aliasing and reduce interpolation error we've applied zero-padding to the projections.

B. NUFFT-based Direct Fourier Method

Based on recent developments connected to the efficient computation of NUFFT –Non Uniform Fast Fourier Transform [9] [10] [11]–, some new algorithms have been proposed which completely avoid the interpolation step.

We've implemented the algorithm suggested by Potts and Steidl [7], using the NFFT C-library developed by Potts and Kunis at the Mathematical Institute of the University of Lübeck –http://www.math.muluebeck.de/potts/nfft/–. The C-function calculating the NUFFT has been embedded in a Matlab *.mex* function.

The algorithm basically flows in two steps: first the 1D FFT of the filtered projections calculated with a given oversampling factor (zero padding the projections)

gives a conventional oversampled polar grid and then 2D inverse NUFFT is applied directly to this sample pattern.

The projections have been filtered with a Shepp-Logan window in the Fourier domain.

IV. Fourier reconstruction methods for divergent projections

Unfortunately, since Fourier slice theorem applies just to parallel projections, the described Fourier reconstruction methods don't match the case of divergent geometry.

There are two possible ways to apply Fourier reconstruction methods to divergent projections. The first way includes a pre-reconstruction step called rebinning which will be described below and allows to obtain parallel projections from the divergent projection data set by interpolation. Once obtained a complete set of parallel projections a any direct Fourier method can be simply applyed.

The second way is to develop a Fourier reconstruction method to be applied directly to the divergent data set. We'll describe a DFM to be applied directly to divergent projections (without any rebinning and interpolation), that we've developed based on the NUFFT.

A. Rebinning

Rebinning is a well known interpolation process that has been employed in the first divergent beam CT scanners until the advent of reconstruction methods dedicated to that geometry (fan beam filtered backprojection). Since interpolation is performed in the projection domain, it is not a critical operation like it is in the Fourier domain and can even be performed linearly without introducing noticeable error.

Comparing equations 1 and 3, we see that the parameters of a ray in the parallel geometry are related to the parameters of the corresponding ray in the divergent geometry by the simple equations:

$$\beta = \theta - \gamma \tag{5}$$

$$\gamma = -\arcsin\frac{s}{r}. \tag{6}$$

Thus, to each sinogram sample to be computed corresponds a point in the space of the divergent projections which value can be evaluated through interpolation. It's interesting to notice that to a line of sinogram samples corresponds a line of points slanted -45^o in the divergent projections space (figure 6).

Has to be pointed out that in order to obtain a complete sinogram for $\theta \in [\Theta, \Theta + \pi]$, at least divergent projections with $\beta \in [\Theta - \Gamma/2, \Theta + \pi + \Gamma/2]$ has to be known.

B. NUFFT based Direct Fourier Method for divergent projections

Given a divergent projection data set, we can reorganize the samples in classes based on the inclination

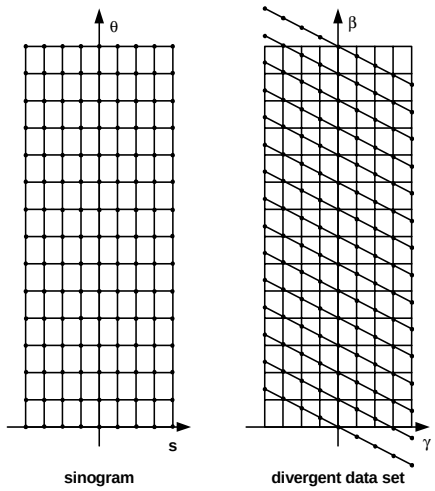

Figura 6 - Rebinning process: dots represent the desired sinogram sample points and the corresponding interpolated points in the divergent projections space.

$\theta = \beta + \gamma$ of the corresponding projection ray. This can be done by dividing the interval $[0, \pi[$ in a number N of sub-intervals equal to the desired number of parallel projections and taking as a parallel projection $j = 1...N$ the set of samples with θ in the j^{th} subinterval. Since such a projection will contain non uniformly distributed samples, to each sample in a projection will be associated the value of the parameter s of the corresponding projection ray.

Applying one dimensional NUFFT to each of these sample sets we can obtain samples on the polar grid in the 2D Fourier space and the algorithm can follow the same way like in the case of parallel projections.

Our implementation of the method flows in the following steps:

- filter of the divergent projections with a Shepp Logan window in Fourier space
- zero padding of the projections
- reorganization of the divergent sample set in parallel projection sample sets
- 1D NUFFT obtaining samples on a conventional oversampled polar grid in the Fourier space
- 2D NUFFT applied to the polar samples.

As will be shown in section (examples) the quality of the reconstructed image is similar to the one obtained with parallel projection, however, this method is computationally expensive due to the sample reorganization step.

V. Fourier projection method

Direct Fourier method can also be applied in the reverse order allowing for the calculation of projection data sets from a digital sample object. We've implemented a Fourier projection method which flows in three steps:

- 2D Fourier transform (through FFT) of the zero-padded image

Figura 7 - Modified Shepp Logan phantom

- Cartesian to polar interpolation
- 1D discrete inverse Fourier transform (through FFT algorithm) of the radial segments od the polar grid obtaining the parallel projections.

Despite of the error due to interpolation in the Fourier domain, Fourier projection method (which is very fast) has been used in iterative reconstruction methods in order to speed up the reprojection step Fessler [12]. Approaches similar to those described for the reconstruction methods can be used in order to reduce the interpolation error.

VI. Some examples

In order to have an idea of the effectiveness of the described algorithms, when compared with the commonly used FBP algorithm, we've performed some simulations using the Modified Shepp-Logan phantom as a model of an object's transversal section (fig. 7).

The simulator, both projection and reconstruction processes, has been implemented in Matlab. In the parallel geometry case 256 projections (255 rays each) over 180^ohave been calculated, while in the divergent geometry case 512 projections over 360^o(255 rays each).

The reconstruction error has been quantitatively evaluated measuring the distance between the original and the reconstructed images. For this purpose we've used the distance metrics proposed by Herman (d- normalized root mean squared distance, r- normalized mean absolute distance, e- worst case distance measure) applied to the region of interest of the images.

In figure 8 some images are shown obtained with different reconstruction methods applied on the same parallel projection data set and in table I are summarized the results of the reconstruction error evaluation. At a first glance it's clear that the quality of the DFM with simple two dimensional linear interpolation in the Fourier space is unacceptable but it significantly improves both qualitatively and quantitatively with the introduction of zero padding of the projections and cubic interpolation in the Fourier space. Moreover, the result obtained with the NUFFT-based method is qualitatively and quantitatively satisfactory and comparable to the result obtained by FBP.

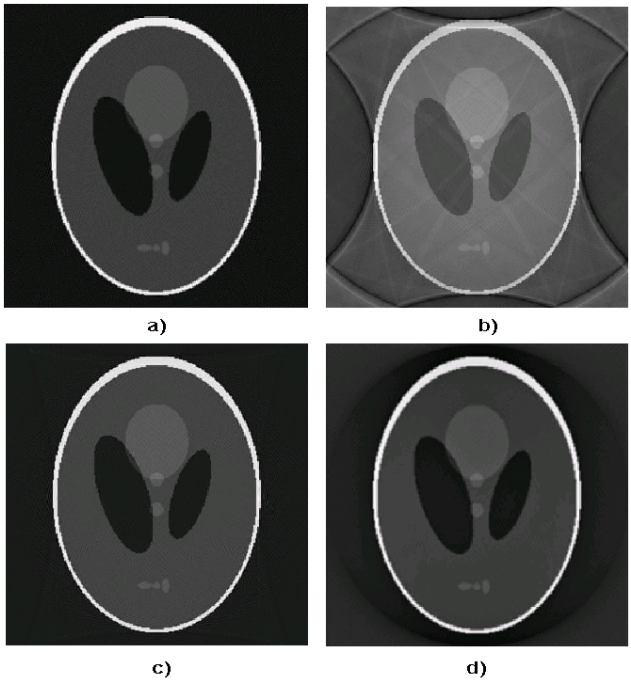

Figura 8 - Images obtained with different reconstruction methods from parallel projection data set: a) filtered backprojection; b) direct Fourier method with linear interpolation in the Fourier space; c) direct Fourier method with zero padding of the projections and linear interpolation in the Fourier space; d) direct Fourier method with zero padding of the projections and cubic interpolation in the Fourier space.

The behaviour of the different methods can be grafically evaluated in figure 9 where the diagonal profile of the reconstructed images and of the original one are compared. Also in this case the good quality of the images reconstructed with DFM with zero padding and cubic interpolation and with the NUFFT method is confirmed.

The last column of table I summarizes the reconstruction time of the different methods and shows how Fourier based methods are impressively faster than the commonly used FBP method.

The results obtained with the corresponding reconstruction methods applied to the divergent projection data set are shown in figure 10 and compared in table II. In this case the FBP method (DBFBP stands for "divergent beam filtered backprojection") and the NUFFT method are applied directly to the divergent beam data set while the other two methods are preceed by a rebinning step and are applied on the synthesized parallel projection dat set. From the perceptual point of view the obtained images do not show any remarkable difference with respect to those of figure 8. The quantitative evaluation of the reconstruction error does confirm the perceptual analysis, showing that the rebinning step, prior to reconstruction, doesn't affect image quality. The only item that differs from the corresponding in the parallel beam case is the reconstruction time which increment, in the case of Fourier based methods, corresponds to the rebinning time

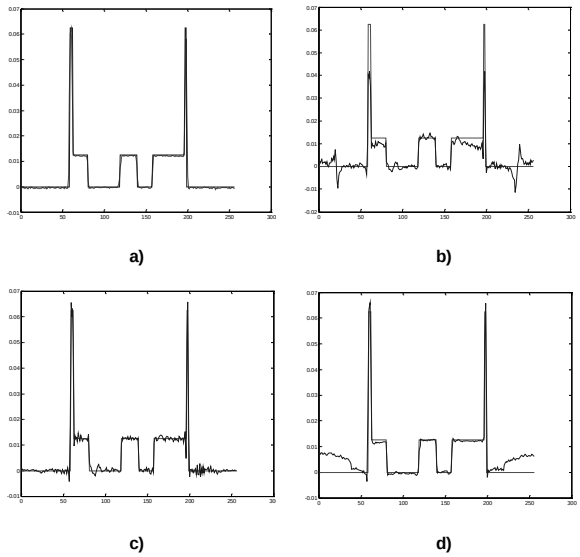

Figura 9 - Comparison between the diagonal of the original image and the diagonals of the reconstructed ones. a) original to FBP. b) original to DFM. c) original to DFM with zero padding. d) original to DFM with zero padding and cubic interpolation in the Fourier space.

while, in the DBFBP case, is due to the larger amount of data to be processed (our implementation of DBFBP, which considers all the views corresponding to a 360^orotation of the focus, can be improved considering just the views corresponding to $180^o + \Gamma$ rotation of the focus). Also in this case, the Fourier based methods show an impressive reduction of reconstruction time.

The projection process in presence of noise has been simulated modeling noise as a Poisson process [13], which depends from the power of the generated beam (N_{in} is the number of incoming photons). The quality of the images reconstructed from noisy projections ($N_{in} = 10^4$) is summarized in tables IV and III. The results show that the performance of the methods degrades similarly in presence of noise and that the rebinning step doesn't affect the quality of the reconstructed image.

VII. Conclusions

Some direct Fourier methods have been implemented and their performance (in ideal and noisy conditions) and has been compared with the performance of the classical FBP method. The results have been analysed qualitatively and quantitatively showing that direct Fourier reconstruction methods are a valid alternative to the commonly used FBP algorithm with a remarkable reduction in computation time.

VIII. Acknowledgement

The autors expecially thank Dr. Daniel Potts and Dr. Stefan Kunis for delivering the NFFT package and for the technical support.

This work is being financially supported by *FCT - Fundação para a Ciência e Tecnologia-*.

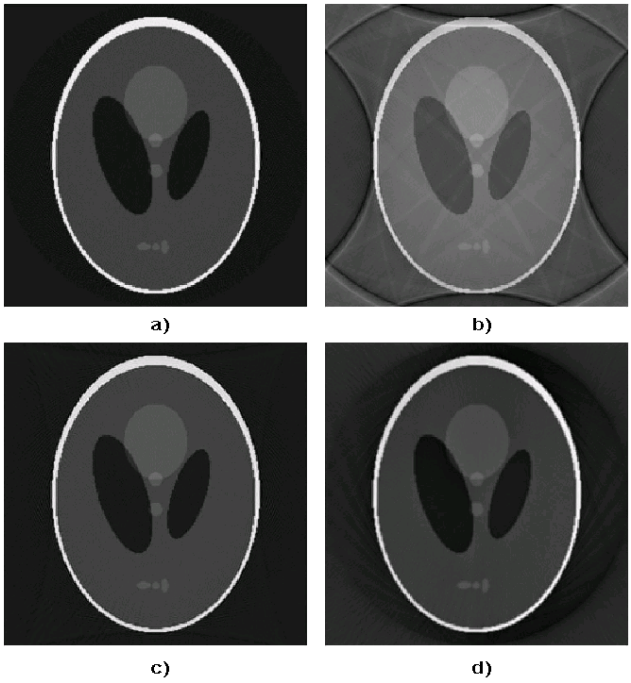

Figura 10 - Images obtained with different reconstruction methods from divergent projection data set: a) filtered backprojection; b) rebinning + direct Fourier method with linear interpolation in the Fourier space; c) rebinning + direct Fourier method with zero padding of the projections and cubic interpolation in the Fourier space; d) NUFFT based direct Fourier method with zero padding of the projections and Shepp Logan filter in the Fourier space.

Referências

[1] A. C. Kak and M. Slaney, *Principles of Computerized Tomographic Imaging*, IEEE Press, 1988.

[2] F. Natterer, *The Mathematics of Computerized Tomography*, Wiley, J., 1986.

[3] F. Natterer and F. Wubbeling, *Mathematical Methods in image reconstruction*, SIAM Monographs on Mathematical Modeling and Computation. SIAM, Society for Industrial and Applied Mathematics, Philadelphia, 2001.

[4] R. M. Lewitt, "Reconstruction algorithms: transform methods", *Proceedings of the IEEE*, vol. 71, no. 3, pp. 390–408, 1983.

[5] F. Natterer, "Fourier reconstruction in tomography", *Numer. Math.*, vol. 47, pp. 343–353, 1985.

[6] M. Magnusson, *Linogram ad other direct Fourier methods for tomographic reconstruction*, Phd, University of Linköping, 1993.

[7] D. Potts and G. Steidl, "New Fourier reconstruction algorithms for computerized tomography", in *SPIE's International Symposium on Optical Science and Technology: Wavelet Applications in Signal and Image Processing VIII*, A. Aldroubi, A. F. Laine, and M. A. Unser, Eds., S. Diego (CA), 2000, vol. 4119, pp. 13–23, SPIE.

[8] K. Fourmont, "Non-equispaced fast Fourier transforms with applications to tomography", *pre-print*, 2000.

[9] A. Dutt and V. Rokhlin, "Fast Fourier transforms for nonequispaced data", *SIAM J. Sci. Comput.*, vol. 14, no. 6, pp. 1368–1393, 1993.

Method \ Distance measure	d	r	e	time (sec.)
FBP (Ram-Lak filter)	0.1643	0.0737	0.0143	46.14
DFM linear int.	0.3996	0.2332	0.0400	0.83
DFM z. pad. cubic int.	0.1183	0.0755	0.0070	6.64
NUFFT-DFM z. pad.	0.1787	0.1108	0.0108	6.76

Tabela I

Quality of images reconstructed from parallel projection data set (fig. 13).

Method \ Distance measure	d	r	e	time (sec.)
DBFBP (Ram-Lak filter)	0.1271	0.0683	0.0077	203.94
DFM linear int. (*)	0.4085	0.2351	0.0401	1.98
DFM z. pad. cubic int. (*)	0.1378	0.0692	0.0093	7.69
NUFFT-DFM z. pad.	0.1941	0.1119	0.0164	46.08

Tabela II

Quality of images reconstructed from divergent projection data set (fig. 15).

Method \ Distance measure	d	r	e
FBP (Ram-Lak filter)	0.1793	0.1125	0.0154
DFM linear int.	0.4080	0.2601	0.0408
DFM z. pad. cubic int.	0.1545	0.1323	0.0069
NUFFT-DFM z. pad.	0.2419	0.2086	0.0167

Tabela III

Quality of images reconstructed from noisy parallel projection data set ($N_{in} = 10^4$).

Method \ Distance measure	d	r	e
DBFBP (Ram-Lak filter)	0.1375	0.1006	0.0074
DFM linear int. (*)	0.3901	0.2525	0.0392
DFM z. pad. cubic int. (*)	0.1574	0.1150	0.0097
NUFFT-DFM z. pad.	0.1995	0.1261	0.0163

Tabela IV

Quality of images reconstructed from noisy divergent projection data set ($N_{in} = 10^4$).

[10] A. F. Ware, "Fast approximate Fourier transforms for irregularly spaced data", *SIAM Rev.*, vol. 40, no. 4, pp. 838–856, 1998.

[11] D. Potts, G. Steidl, and M. Tasche, "Fast Fourier transforms for nonequispaced data: a tutorial", in *Modern sampling theory: mathematics and applications*, J. J. Benedetto and P. J. S. G. Ferreira, Eds., Applied and Numerical Harmonic Analysis Series, pp. 249–274. Birkhauser, Boston, 2001.

[12] J. A. Fessler, "Iterative tomographic image reconstruction using nonuniform fast Fourier transforms", Technical report, Comm. and Sign. Proc. Lab., Dept. of EECS, Univ. of Michigan, December 2001 2001.

[13] S. De Francesco and A. M. F. d. Silva, "Multi-slice spiral CT simulator for dynamic cardio-pulmonary studies", in *Medical Imaging 2001: Physiology and Function from Multidimensional Imaging*, A. V. Clough and C.-T. Chen, Eds., S. Diego, 2002, vol. 4683, pp. 305–316, SPIE.